

Multi-Objective Reinforcement Learning for Power Grid Topology Control

Thomas Lautenbacher
50Hertz Transmission GmbH
Berlin, Germany
thomasrene.lautenbacher@50Hertz.com

Ali Rajaei
Delft University of Technology
Delft, The Netherlands
a.rajaei@tudelft.nl

Davide Barbieri
TenneT TSO B.V.
Arnhem, The Netherlands
davide.barbieri@tennet.eu

Jan Viebahn
TenneT TSO B.V.
Arnhem, The Netherlands
jan.viebahn@tennet.eu

Jochen L. Cremer
Delft University of Technology
Delft, The Netherlands
j.l.cremer@tudelft.nl

Abstract—Transmission grid congestion increases as the electrification of various sectors requires transmitting more power. Topology control, through substation reconfiguration, can reduce congestion but its potential remains under-exploited in operations. A challenge is modeling the topology control problem to align well with the objectives and constraints of operators. Addressing this challenge, this paper investigates the application of multi-objective reinforcement learning (MORL) to integrate multiple conflicting objectives for power grid topology control. We develop a MORL approach using deep optimistic linear support (DOL) and multi-objective proximal policy optimization (MOPPO) to generate a set of Pareto-optimal policies that balance objectives such as minimizing line loading, topological deviation, and switching frequency. Initial case studies show that the MORL approach can provide valuable insights into objective trade-offs and improve Pareto front approximation compared to a random search baseline. The generated multi-objective RL policies are 30% more successful in preventing grid failure under contingencies and 20% more effective when training budget is reduced - compared to the common single objective RL policy.

Index Terms—Transmission network topology control, Multi-objective reinforcement learning, Deep optimistic linear support.

I. INTRODUCTION

The energy transition and the shift toward renewable energy sources are crucial steps for mitigating climate change and ensuring a sustainable energy future. However, this transition poses significant operational challenges for system operators, including congestion management. Transmission network topology control is an under-utilized and non-costly source of flexibility. Adjusting the network topology, such as line switching or modifying busbar connections within substations, can reroute power flows to prevent line overloads and mitigate cascading outages [1]–[3]. In addition to maintaining continuous electricity supply, power systems must address other objectives, such as minimizing asset wear, reducing operational cost, and mitigating environmental impacts. Achieving these objectives requires a multi-objective approach to decision-

making that maintains grid security while addressing other operational objectives [4].

Transmission network topology control problem can be modeled as a mixed-integer non-linear optimization problem which is computationally challenging to approach. The so-called combinatorial explosion of possible topologies and the complex nonlinear nature of power systems [1] makes this problem challenging. To address these challenges, heuristic and expert rule-based approaches, such as in [5]–[8] are developed to determine corrective topological actions to relieve congestion. However, these approaches do not provide a sequence of control actions and may lead to sub-optimal solutions. To provide sequences of actions, recently researchers explored the use of reinforcement learning (RL) and Artificial Intelligence (AI) more broadly for topological control [3], [9]–[11]. Studies such as [12]–[15] explore RL-based approaches, including the deep duelling Q-network (DDQN) initialized with imitation learning [12], the Semi-Markov actor-critic algorithm [13], the cross-entropy method with importance sampling [14], and the proximal policy optimization (PPO) [15]. Additionally, [16] develops an AlphaZero-based approach using Monte-Carlo tree search to simulate future outcomes, and guide the agent toward long-term strategies, while [17] presents a curriculum-based approach to improve learning efficiency and stability. Building on these ideas, [18] combines curriculum learning with tree search to benefit from long-term strategies as well as the efficiency and stability. Some studies focus on addressing the combinatorial explosion of the topology control problem through hierarchical RL [19] and multi-agent RL [20]. Furthermore, [21] proposes a reward design using multiple metrics to reduce overloads. However, the developed approaches in [5]–[8], [12]–[21] focus on single operational objectives and providing only a single policy. This limits their application to address the trade-offs inherent in the multi-objective nature of power systems and to provide a set of policies for operators to select from.

This paper proposes a multi-objective RL (MORL) approach to address the network topology control problem. Despite

The research was carried out for an MSc thesis project in Delft University of Technology.

previous studies on RL approaches, to the best of the authors' knowledge, a multi-policy MORL approach for topology control has not been investigated before. To this end, we implement deep optimistic linear support (DOL) and multi-objective PPO (MOPPO) to generate a set of Pareto-optimal policies. Additionally, we develop custom reward functions for different operational objectives, including line loading, topological deviation, and switching frequency. The proposed MORL approach not only shows the trade-offs between these objectives but also provides a set of policies that balance these trade-offs, offering a decision-support approach for system operators. By considering multiple rewards, the approach effectively relieves grid congestion while addressing other operational objectives.

The rest of the paper is organized as follows. Section II presents the proposed MORL approach and the design of the reward functions. Section III presents the case studies, investigating the efficiency and robustness of the proposed approach. Section IV provides discussions and concludes the paper.

II. METHODOLOGY

This paper aims to provide a decision-support approach for transmission system operators to perform topological control considering multiple objectives. The proposed approach integrates a multi-objective adaptation of the PPO algorithm [22], [23] (MOPPO) with deep optimistic linear support [24]. To capture different operational objectives, we design custom reward functions that address line loading, topological deviation and switching frequency. The proposed approach considers a multi-policy MORL [25], which results in a set of optimal solutions rather than a single solution. This allows system operators to better understand the trade-offs among objectives and select the most appropriate policy. Fig. 1 depicts the proposed approach. By using DOL as an outer loop method within the MORL approach, the convex coverage set of solutions is constructed iteratively. In each iteration, the DOL generates a new set of weight vectors \mathbf{w} and gives one weight vector with the highest priority to MOPPO, that is then trained in the multi-objective environment. MOPPO uses \mathbf{w} to account for the multiple rewards \mathbf{R}_t . After training, the MOPPO is evaluated. If the average value vector over the evaluation episodes \mathcal{V} , found by the MOPPO, is Pareto optimal, it is added to the convex coverage set (CCS). The detailed methodology is explained in the following.

A. Single-Policy Multi-Objective PPO

In order to learn on multiple rewards, the agent needs to receive a reward signal for each of the objectives. To this end, we extend the original RL grid environment into a multi-objective environment, allowing the agent to receive a d -dimensional reward vector $\mathbf{r}_t \in \mathbb{R}^d$, where d is the number of objectives. In this paper, the rewards reflect the operational objectives of reducing the line loading, decreasing the topological deviation, and reducing the switching frequency, explained in detail in section II-B.

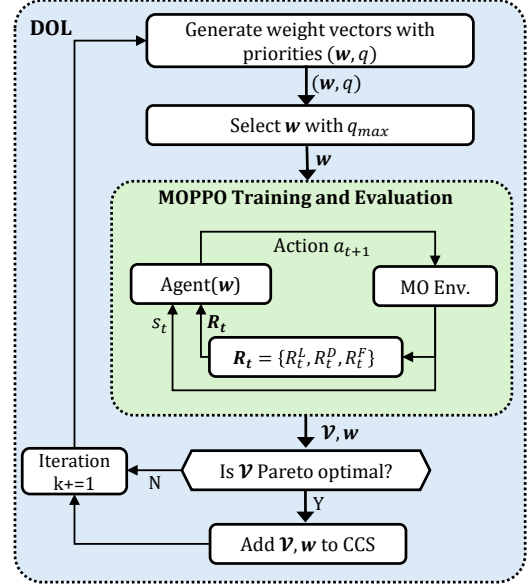


Fig. 1: Schematic of the proposed MORL approach with deep optimistic linear support.

At the core of the proposed approach is the MOPPO Algorithm 1, which is trained using a reward vector \mathbf{r}_t from the environment and a weight vector \mathbf{w} , serving as a scalarization, from the DOL to deliver a single policy solution [23]. The MOPPO algorithm processes the d -dimensional reward vector \mathbf{r}_t by using a d -dimensional critic head, resulting in a vectorized value function for each state s :

$$\mathbf{V}^\pi(s_t) = \mathbb{E}_\pi \left[\sum_{t=0}^{\infty} \gamma^t \mathbf{r}_t \mid s_t = s \right], \quad (1)$$

where $\mathbf{V}^\pi(s) \in \mathbb{R}^d$ is the vectorized state-value function per state s under policy π , $\mathbf{r}_t \in \mathbb{R}^d$ is the vector of rewards at time t , and $\gamma \in [0, 1)$ is the discount factor.

The vectorized advantages $\mathbf{A}_t \in \mathbb{R}^d$ are then calculated using generalized advantage estimation (GAE) [22]. These advantages are then scalarized using a weighted sum approach:

$$A_t = \mathbf{w}^\top \mathbf{A}_t, \quad (2)$$

where $\mathbf{w} \in \mathbb{R}^d$ is the weight vector representing the scalarization preferences, satisfying $\sum_{i=1}^d w_i = 1$ for $w_i \geq 0$, and $A_t \in \mathbb{R}$ is the scalarized advantage. This step incorporates the scalarization function, given by DOL, to train the single-policy MOPPO. The scalarized advantage is then used to calculate the policy loss, which contributes to the total loss. For detailed information on the loss calculation in MOPPO, we refer to [23]. The MOPPO produces the final value vector \mathbf{V} and the model m , containing the neural network weights θ and the learnt policy π .

B. Reward functions for operational objectives

1) *Line Loading Reward*: The *L2RPNReward*, referred to here as *Line Loading Reward*, is the conventional reward

Algorithm 1 Multi-Objective PPO (MOPPO) Training

Require: Multi-Objective MDP, scalarization weight vector \mathbf{w} , number of update cycles

- 1: initialize MOPPO network $\theta \leftarrow \emptyset$
- 2: **for** Number of updates cycles **do**
- 3: initialize replaybuffer(B) batch $\mathbb{B} \leftarrow \emptyset$
- 4: $(\mathbf{V}_t, \mathbf{R}_t)_{\mathbb{B}} \leftarrow \text{collect_samples}(\text{MOPPO}\theta)$
{Fill replay buffer \mathbb{B} by collecting samples from the environment, containing batchsize tuples of vectorized value function and vectorized rewards $(\mathbf{V}_t, \mathbf{R}_t)_{\mathbb{B}}$ }
- 5: $\mathbf{A}_t \leftarrow \text{compute_advantages}((\mathbf{V}_t, \mathbf{R}_t)_{\mathbb{B}})$
- 6: $A_t = \mathbf{w}^\top \mathbf{A}_t$ {Scalarize advantages (2)}
- 7: $\theta \leftarrow \text{update}(A_t)$ {updates the neural network}
- 8: **end for**

used in the L2RPN competition [3], and widely adopted as a default reward in the literature [7], [8], [19], [20]. This reward emphasizes maintaining adequate thermal loading margins on power lines to ensure grid security. For each power line l , the thermal loading margin is defined:

$$\text{Margin}_{l,t} = \begin{cases} \frac{\bar{F}_l - |F_{l,t}|}{\bar{F}_l} & \text{if } |F_{l,t}| \leq \bar{F}_l \\ 0 & \text{if } |F_{l,t}| > \bar{F}_l \end{cases} \quad (3)$$

where \bar{F}_l is the thermal limit (ampacity) of line l , and $|F_{l,t}|$ is the absolute value of the current flow in amps. The line loading reward R_t^L at each time step is calculated as:

$$R_t^L = \sum_{l=1}^L (\text{Margin}_{l,t})^2 \quad (4)$$

where, L represents the total number of power lines. This reward function encourages the agent to keep the power flows within the thermal limits of the lines, penalizing situations where lines are overloaded.

2) *Topological Deviation*: This reward assigns a penalty based on the degree of deviation of the current grid topology from its initial, default configuration [26]. In the default state, all the busbar coupler switches are closed, resulting in a fully meshed configuration and a single electrical node per substation. The reward decreases progressively as the topology deviates from this configuration, encouraging the agent not to deviate too far from the original topology [4].

At each time step t , we define the topological deviation for a substation i as:

$$D_{i,t} = \begin{cases} 1, & \text{if any element in substation } i \\ & \text{is assigned to a different bus,} \\ 0, & \text{otherwise.} \end{cases} \quad (5)$$

The total topological deviation at time t is :

$$D_t = \sum_{i=1}^N D_{i,t} \quad (6)$$

where N denotes the total number of substations.

The Deviation reward at time t is:

$$R_t^D = \begin{cases} r_{\text{default}}, & \text{if } D_t = 0, \\ r_{\text{minor}}, & \text{if } D_t \leq d_{\text{threshold}}, \\ r_{\text{major}}, & \text{otherwise,} \end{cases} \quad (7)$$

where r_{default} is a positive reward indicating the maintenance of the default state, r_{low} is a small penalty for minor deviations from the default configuration, r_{high} is a larger penalty for significant deviations, and $d_{\text{threshold}}$ is the predefined threshold for minor deviations.

Transmission networks operate more securely and more resilient to disturbances in a fully meshed configuration with minimal or no changes to the topology [3]. Consequently, the piecewise linear design of the reward functions incentivizes the agent not to minimize deviation from the default configuration by imposing disproportionately higher penalties for significant alterations to the grid topology.

3) *Switching Frequency*: This reward penalizes the number of switching actions within a specified time interval, aiming to discourage instability from frequent adjustments [4]. To prevent the reward from exploding, we consider only the accumulated switching actions within one time interval. Thus, the total possible episode is divided into intervals $\{\mathcal{T}_m\}$ (e.g., timesteps within one hour or within one day). At each RL time step t , the cumulative switching actions F_t in interval $\{\mathcal{T}_m\}$ is computed as:

$$F_t = \sum_{t \in \mathcal{T}_m} \text{switching actions in interval } m \text{ up to } t \quad (8)$$

The switching frequency reward is defined as:

$$R_t^F = \begin{cases} r_{\text{DoNothing}}, & \text{if } F_t = 0, \\ r_{\text{low}}, & \text{if } F_t \leq F_{\text{low}}^{\text{th}}, \\ r_{\text{high}}, & \text{if } F_t \geq F_{\text{high}}^{\text{th}}, \end{cases} \quad (9)$$

where r_{default} is a baseline reward indicating no switching actions, r_{low} is a penalty for low switching frequency, r_{high} is a penalty for high switching frequency, and $F_{\text{low}}^{\text{th}}, F_{\text{high}}^{\text{th}}$ are the predefined thresholds for low and high switching frequencies, respectively.

C. Deep Optimistic Linear Support

To generate a set of policies, we employ the deep optimistic linear support (DOL) algorithm to iteratively construct the optimal solution set of policies [24]. DOL functions as an outer-loop MORL approach [25], leveraging optimistic linear support (OLS) [27] to iteratively construct the convex coverage set (CCS) of a multi-objective problem by generating scalarization functions in the form of weight vectors \mathbf{w} and updating the solution set Ω^s accordingly [25]. Additionally, here DOL facilitates integration of MOPPO as a multi-objective single policy RL Algorithm.

Algorithm 2 provides details of the proposed DOL approach. In the first iteration, DOL assigns the extrema weights to the queue with infinite priority, ensuring these weights are processed first by the MOPPO algorithm (line 7). For each

Algorithm 2 Deep Optimistic Linear Support (DOL)

Require: single-policy RL algorithm MO PPO, maximum number of iterations k^{max} , reuse option (no reuse, full reuse, partial reuse)

- 1: Initialize partial CCS $\Omega^s \leftarrow \emptyset$
- 2: Initialize set of visited weights $W \leftarrow \emptyset$
- 3: Initialize priority queue $Q \leftarrow \emptyset$
- 4: Initialize model repository Models $\leftarrow \emptyset$
- 5: Initialize iteration k as 0.
- 6: **for all** extremum weight w_e of the weight simplex **do**
- 7: Add (w_e, ∞) to Q {Add extrema with infinite priority}
- 8: **end for**
- 9: **while** Q is not empty **and** $k < k^{max}$ **do**
- 10: Pop w from Q with the highest priority q_{max}
- 11: **if** reuse option is no reuse **or** Models is empty **then**
- 12: Initialize model parameters θ randomly
- 13: **else**
- 14: Find the closest weight $w_{closest}$ in W to w
- 15: Initialize model parameters θ with parameters from Models[$w_{closest}$]
- 16: **if** reuse option is partial reuse **then**
- 17: Randomly reinitialize the last layer of the model
- 18: **end if**
- 19: **end if**
- 20: $\theta_{new} \leftarrow$ MO PPO(m, w, θ) {Train RL algorithm with weight w }
- 21: $\mathcal{V} \leftarrow$ MO PPO(m, w, θ_{new}) {Evaluate RL algorithm with weight w }
- 22: $W \leftarrow W \cup \{w\}$
- 23: **if** there exists w' such that $w' \cdot \mathcal{V} > \max_{U \in \Omega^s} w' \cdot U$ **then**
- 24: Remove corner weights made obsolete by \mathcal{V} from Q , store them in W_{del}
- 25: $W_{del} \leftarrow W_{del} \cup \{w\}$
- 26: $\Omega^s \leftarrow \Omega^s \cup \{\mathcal{V}\}$
- 27: Remove vectors from Ω^s that are no longer optimal after adding \mathcal{V}
- 28: Models[w] $\leftarrow \theta_{new}$
- 29: $(W_{new}, q_{new}) \leftarrow$ newCornerWeights(Ω^s, V)
- 30: **end if**
- 31: $k+ = 1$
- 32: **end while**
- 33: **return** Ω^s and the models in Models {models correspond to the policies implicitly integrated in the neural network weights}

new iteration of the DOL algorithm, the weight vector with the highest priority q_{max} (expected highest improvement) will be given to the MOPPO (line 10). The MOPPO is trained using w , described in Algorithm 1. The trained agent containing θ_{new} is evaluated and produces \mathcal{V} as the average value vector across the evaluation episodes (line 21). \mathcal{V} is used to evaluate if the trained model contributes to the CCS. \mathcal{V} is the sampled vectorized value-estimation $\mathbf{V}(s)$ over the evaluation episodes, based on the received rewards; hence, \mathcal{V} does not necessarily

Algorithm 3 Selection Process for Best Performing Policy

Require: Set of policies $\{\pi_1, \pi_2, \dots, \pi_n\}$, set of episode durations $\{E_1, E_2, \dots, E_n\}$, extrema weights $\{w_e\}$

- 1: Initialize best policy $\pi^{MO} \leftarrow \emptyset$
- 2: Initialize maximum episode duration $E^{max} \leftarrow 0$
- 3: **for all** $i \in \{1, 2, \dots, n\}$ **do**
- 4: Retrieve policy π_i and corresponding episode duration E_i
- 5: **if** π_i is not trained on extrema weights $\{w_e\}$ **and** $E_i > E^{max}$ **then**
- 6: $E^{max} \leftarrow E_i$
- 7: $\pi^{MO} \leftarrow \pi_i$
- 8: **end if**
- 9: **end for**
- 10: **return** π^{MO}

reflect the vectorized state dependent value function $\mathbf{V}(s)$ (1).

If the new value vector improves the coverage set Ω^s , obsolete corner weights are deleted, the new value vector is added to the set, the model is saved and new corner weights are calculated (line 23-29). To determine next weight vectors, corner weights are identified as the weights where the piecewise-linear convex (PWLC) surface of $\mathcal{V}(w)$ changes slope (line 29). Specifically, these corner weights are the vertices of the polyhedral subspace above $\mathcal{V}(w)$. The priority of the new corner weights is calculated based on their distance to the assumed optimistic upper bound of the CCS. Details on the newCornerWeights are provided in [27]. The original stopping criterion, which depended on a minimum improvement in the CCS [24], is replaced with a predefined maximum number of iterations, k^{max} (line 9). This allows for an initial estimate of the training effort by fixing the number of iterations in advance.

DOL offers the possibility of reusing model parameters from the nearest model (lines 11-19). The neural network weights θ from the model with the closet w are used to initialize the next MOPPO. For a detailed view on DOL and OLS, we refer to [24] and [27], respectively.

D. Policy Selection

Despite the multi-objective nature of the problem, the ultimate goal of the system operator is maintain secure system operation as long as possible [4]. To this end, Algorithm 3 is proposed to identify the best-performing policy as a recommendation for the system operator. We assess policy quality using a metric independent of the rewards, referred to as *Episode Duration* (E) [26]. E measures how long the agent can prevent the power system from premature grid failure. After generating the complete set of policies, we select the best-performing policy (π^{MO}) for each seed run based on (E). Policies trained solely on extreme weights are excluded from consideration, as the focus is on selecting policies optimized for multiple rewards.

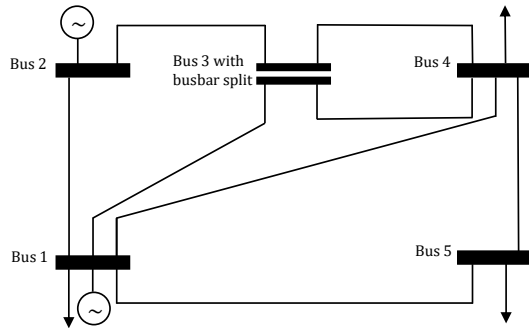


Fig. 2: Schematic of the RTE 5-bus system with busbar splitting on substation 3.

III. CASE STUDIES

A. Settings

All case studies are performed on the RTE 5-bus system in the Grid2Op environment [26], providing initial insights into a MORL approach for topology control. Figure 2 shows the 5-bus system. Each environment scenario lasts a week with a 5-min resolution (2016 time steps), which corresponds to the maximum episode duration (E). We use 16 scenarios for training, 2 scenarios for validation, and 2 scenarios for testing. The experiments are performed on up to 20 random seeds initializing the environment. The PPO neural network architecture consists of 2 fully connected layers with 64-dimensional hidden features. Training is performed using the Adam optimizer with a learning rate of 5×10^{-4} and a batch size of 512. The MOPPO algorithm assumes 4 update cycles. In the case study on robustness to contingencies (Section III-C), an adversarial agent is considered to simulate N-1 contingency states by randomly targeting power lines. Additionally, a set of common expert rules are considered to improve the performance and ensure safety, as detailed in [8], [14]. All computations are performed using DelftBlue’s super-computer, equipped with Intel XEON E5-6248R 24C 3.0GHz CPU cores [28]. We use Grid2Op 1.10, LightSim2Grid 0.8, pandapower 2.14, gymnasium 0.29, mo-gymnasium 1.1 and the morl-baselines 1.0 package. The code for this study is publicly available in [29].

In Section III-B, we compare our approach to a random sampling (RS) benchmark, which replaces the DOL component by randomly selecting weight vectors from a uniform distribution. These randomly selected weights are then provided to the MOPPO, following the same process as in the DOL-based approach. To enhance this baseline, we incorporate the extrema weights [27], as exploring these weights is expected to yield significant gains in the objective space.

B. Pareto Front Approximation

Table I presents the results for hypervolume, sparsity and inverted generational distance (IGD) of the proposed DOL approach and RS. The hypervolume metric evaluates the spread and distribution of the solution space, the sparsity metric quantifies the density of the solution set, and IGD measures how accurately the generated solution set approximates the

Approach	HV	HV	Spa	Spa	IGD	IGD
	Mean	Std	Mean	Std	Mean	Std
DOL	44.62	27.32	0.11	0.04	0.84	0.20
RS	37.35	31.67	0.22	0.06	2.22	0.12

TABLE I: Hypervolume, sparsity and inverted generational distance for DOL and RS Methods.

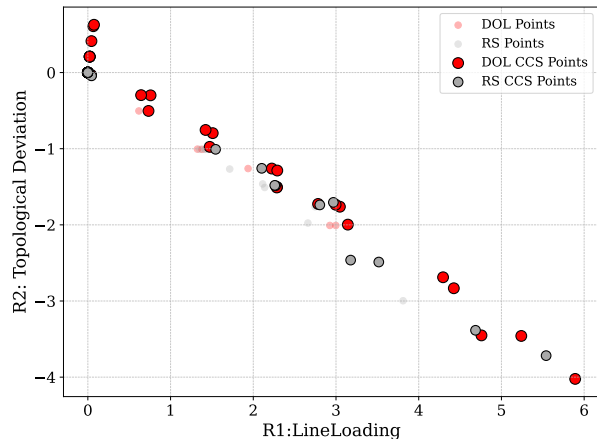


Fig. 3: 2D Projection of Super CCS for line loading reward vs topological deviation Reward.

true Pareto front [25]. The DOL and RS achieve similar mean hypervolume, with DOL slightly outperforming RS. However, DOL shows 50% lower mean sparsity compared to RS, indicating a much denser coverage of the Pareto front, more suitable for a decision support tool. Additionally, DOL exhibits a substantial reduction in IGD by 60%, indicating a better approximation of the assumed true convex coverage set.

Figs. 3 to 5 show the 2D projections of the super CCS for DOL and RS runs across five seeds into 2-dimensional reward spaces. The super CCS is constructed as the convex set over all generated solution sets across all seeds and both DOL and RS generated solutions. The Super CCS here serves as an indicator for the assumed true CCS. The DOL generates more points compared to the RS benchmark that contribute to the formation of the super CCS. Assuming the super CCS reflects the true trade-offs in the objective space, we can conclude that DOL more closely approximates these trade-offs.

Figs. 3 to 5 illustrates key trade-offs among the objectives. In Fig. 3, a clear conflict is observed between R^L and R^D , where reducing topological deviation often results in lower line loading. This indicates that changes in topology are sometimes necessary to maintain grid security, trading off topological deviation for improved line loading.

In Fig. 4, low R^L corresponds to low R^S , indicating that minimal switching interaction allows the grid to operate securely. However, some switching is necessary to further increase R^L . The trade-off solutions in the top middle of Fig. 4 may appeal to power system operators who seek an RL policy balancing low switching frequency with low line loading.

In Fig. 5, R^D and R^S exhibit a trade-off, as lower switching frequency can lead to higher topological deviation. This occurs because deviations in topology persist longer without switch-

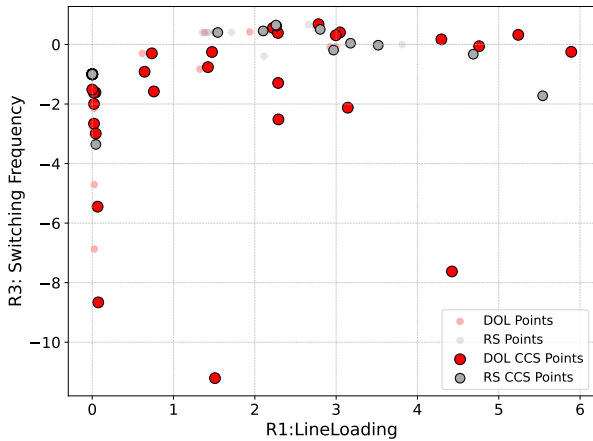


Fig. 4: 2D Projection of Super CCS for line loading reward vs switching frequency reward.

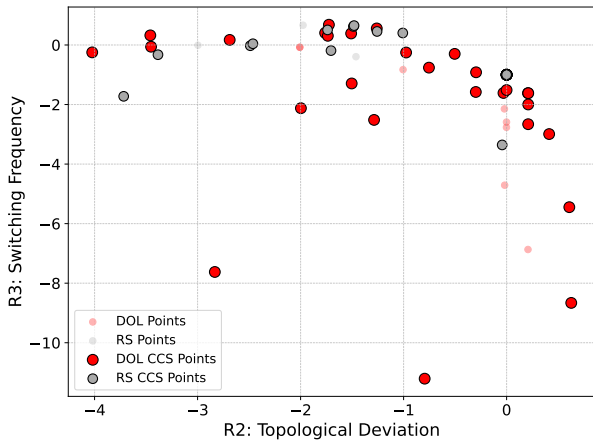


Fig. 5: 2D Projection of Super CCS for topological deviation reward vs switching frequency reward

ing actions, leaving the grid in a deviated state for extended periods.

C. Robustness to N-1 Contingencies

This case study investigates the robustness of MO policies that are trained on multiple rewards compared to SO policies under N-1 contingency states. The contingency states are generated by an adversarial attacker, which disconnects power lines at random. We use the same settings for the adversarial attacks as in [19]. The multi-objective policies (MO policies) are trained on R^L , R^D , and R^F rewards, while the SO policy is trained on the common R^L reward. The MO policies are selected based on Algorithm 3 considering the Episode Duration metric E . The following scenarios are considered:

- No Contingencies: The environment does not include any unplanned contingencies (baseline).
- Moderately Frequent Contingencies: line disconnection randomly at maximum twice a day.
- Highly Frequent Contingencies: line disconnection randomly at maximum four times a day.

Table II compares the mean episode duration (E) and the improved episode duration (ΔE) normalized by the

	N-1 Contingency Frequency		
	No	Moderate	High
$E^{MO}(\%)$	94.83	97.68	90.33
$E^{SO}(\%)$	82.66	58.61	66.47
$\Delta E(\%)$	10.17	39.07	23.86

TABLE II: Comparison of episode duration (E) for multi objective and single objective policies under N-1 contingencies.

	Training Budget		
	Low	Moderate	Full
$E^{MO}(\%)$	95.27	90.44	94.83
$E^{SO}(\%)$	73.39	84.95	82.66
$\Delta E(\%)$	21.88	5.49	10.17

TABLE III: Comparison of episode duration (E) for multi objective and single objective policies under constrained training.

total number of possible steps for the MO and SO policies. The results show that MO RL policies achieve a higher average episode duration. For instance, for highly frequent contingencies, the MO Policies achieve 23.86% increase in episode duration compared to SO policies. In the setting with moderately frequent contingencies, the MO Policies outperform the SO policies by almost 40%. By learning to reduce the topological deviation and to reduce the switching frequency, agents trained with MO policies develop more robust strategies, which perform better under contingencies.

D. Efficient Training

This case study investigates the training efficiency of MO and SO policies when computational resources are limited. Similar to the previous case study, we evaluate performance using the average episode duration and select the best MO policies according to Algorithm 3. Table III compares MO and SO policies considering the following training scenarios:

- Full Training Budget: The agent is trained with the default number of interactions (2048 training samples, 4 update cycles).
- Moderate Training Budget: The agent is trained on 75% of the training (1536 training samples, 3 update cycles).
- Low Training Budget: The agent is trained on 50% of the training (1024 training samples, 2 update cycles).

Table III shows that MO policies outperform SO policies with fewer training iterations. Notably, in the low training scenario, MO policies achieve a 21.88% higher episode duration on average. By focusing on reducing switching frequency and maintaining proximity to the original topology early in training, MO policies develop effective strategies at an earlier stage. As a result, MO policies provide faster and more efficient learning, a critical advantage as the computational complexity of larger grids increases exponentially.

IV. DISCUSSION AND CONCLUSION

This paper presents the first investigation into multi-objective reinforcement learning (MORL) for power grid topology control. We demonstrated trade-offs exist among conflicting operational objectives in the underlying problem

of topological control. From analyzing the initial case studies, we conclude the approach seems promising to alleviate challenges in modeling this topological control problem. In other words, the underlying problem being multi-objective can be approached through learning in a more principled way. The initial case studies show that the proposed DOL approach generates higher-quality solution sets, with higher density and closer approximation of the Pareto frontier, compared to random sampling, thereby offering enhanced decision support and a more comprehensive set of policies for operators to select from. Additionally, by simultaneously reducing topological deviation, switching frequency and line loading, multi-objective policies achieve 24% higher average episode duration under high-contingency scenarios, compared to single-objective policies. The results also show that multi-objective policies improve training efficiency; when using 50% of the training steps, MO policies achieve a 22% better episode duration compared to single-objective policies. However, some limitations of the study can be noted. The 5-bus system used in this research does not fully reflect the complexity of real-world power systems. Future work should adapt the proposed approach to a larger grid to investigate its practical applicability. Additionally, this study focuses on a limited set of operational objectives, including line loading and switching frequency. Future research should explore other objectives, such as operational cost, and environmental impacts. Moreover, expanding MORL for topology control to include both topological actions and generator re-dispatch should be explored in future research.

ACKNOWLEDGMENT

AI4REALNET has received funding from European Union's Horizon Europe Research and Innovation programme under the Grant Agreement No 101119527. Views and opinions expressed are however those of the authors only and do not necessarily reflect those of the European Union. Neither the European Union nor the granting authority can be held responsible for them.

REFERENCES

- [1] M. Heidarifar, P. Andrianesis, P. Ruiz, M. C. Caramanis, and I. C. Paschalidis, "An optimal transmission line switching and bus splitting heuristic incorporating ac and n-1 contingency constraints," *International Journal of Electrical Power & Energy Systems*, vol. 133, p. 107278, 2021.
- [2] A. Ewerszumrode, N. Erle, S. Krahl, and A. Moser, "An iterative approach to grid topology and redispatch optimization in congestion management," *Electric Power Systems Research*, vol. 234, p. 110700, 2024.
- [3] A. Marot, B. Donnot, C. Romero, B. Donon, M. Lerousseau, L. Veyrin-Forrer, and I. Guyon, "Learning to run a power network challenge for training topology controllers," *Electric Power Systems Research*, vol. 189, p. 106635, 2020.
- [4] J. Viebahn, S. Kop, J. v. Dijk, H. Budaya, M. Streefland, D. Barbieri, P. Champion, M. Jothy, V. Renault, and S. Tindemans, "Gridoptions tool: Real-world day-ahead congestion management using topological remedial actions," *CIGRE*, 2024.
- [5] S. Babaeinejadsarookolae, B. Park, B. Lesieutre, and C. L. DeMarco, "Transmission congestion management via node-breaker topology control," *IEEE Systems Journal*, 2023.
- [6] A. Marot, B. Donnot, S. Tazi, and P. Panciatici, "Expert system for topological remedial action discovery in smart grids," in *Mediterranean Conference on Power Generation, Transmission, Distribution and Energy Conversion (MEDPOWER 2018)*. IET, 2018, pp. 1–6.

- [7] I. Hrgović and I. Pavić, "Substation reconfiguration selection algorithm based on ptdfs for congestion management and rl approach," *Expert systems with applications*, vol. 257, p. 125017, 2024.
- [8] M. Lehna, J. Viebahn, A. Marot, S. Tomforde, and C. Scholz, "Managing power grids through topology actions: A comparative study between advanced rule-based and reinforcement learning agents," *Energy and AI*, vol. 14, p. 100276, 2023.
- [9] A. Kelly, A. O'Sullivan, P. de Mars, and A. Marot, "Reinforcement learning for electricity network operation," *arXiv preprint arXiv:2003.07339*, 2020.
- [10] A. Marot, B. Donnot, G. Dulac-Arnold, A. Kelly, A. O'Sullivan, J. Viebahn, M. Awad, I. Guyon, P. Panciatici, and C. Romero, "Learning to run a power network challenge: a retrospective analysis," in *NeurIPS 2020 Competition and Demonstration Track*. PMLR, 2021, pp. 112–132.
- [11] A. Marot, B. Donnot, K. Chaouache, A. Kelly, Q. Huang, R.-R. Hossain, and J. L. Cremer, "Learning to run a power network with trust," *Electric Power Systems Research*, vol. 212, p. 108487, 2022.
- [12] T. Lan, J. Duan, B. Zhang, D. Shi, Z. Wang, R. Diao, and X. Zhang, "Ai-based autonomous line flow control via topology adjustment for maximizing time-series atcs," in *2020 IEEE Power & Energy Society General Meeting (PESGM)*. IEEE, 2020, pp. 1–5.
- [13] D. Yoon, S. Hong, B.-J. Lee, and K.-E. Kim, "Winning the l2rpn challenge: Power grid management via semi-markov afterstate actor-critic," in *International Conference on Learning Representations*, 2020.
- [14] M. Subramanian, J. Viebahn, S. H. Tindemans, B. Donnot, and A. Marot, "Exploring grid topology reconfiguration using a simple deep reinforcement learning approach," in *2021 IEEE Madrid PowerTech*. IEEE, 2021, pp. 1–6.
- [15] A. Chauhan, M. Baranwal, and A. Basumatary, "Powrl: A reinforcement learning framework for robust management of power networks," in *Proceedings of the AAAI Conference on Artificial Intelligence*, vol. 37, no. 12, 2023, pp. 14 757–14 764.
- [16] M. Dorfer, A. R. Fuxjäger, K. Kozak, P. M. Blies, and M. Wasserer, "Power grid congestion management via topology optimization with alphazero," *arXiv preprint arXiv:2211.05612*, 2022.
- [17] A. R. R. Matavalam, K. P. Guddanti, Y. Weng, and V. Ajjarapu, "Curriculum based reinforcement learning of grid topology controllers to prevent thermal cascading," *IEEE Transactions on Power Systems*, 2022.
- [18] G. J. Meppelink, A. Rajaei, and J. L. Cremer, "A hybrid curriculum learning and tree search approach for network topology control," *Electric Power Systems Research*, 2025, accepted.
- [19] B. Manczak, J. Viebahn, and H. van Hoof, "Hierarchical reinforcement learning for power network topology control."
- [20] E. van der Sar, A. Zoeca, and S. Bhulai, "Multi-agent reinforcement learning for power grid topology optimization."
- [21] I. Hrgović and I. Pavić, "Reward design for intelligent deep reinforcement learning based power flow control using topology optimization," *Sustainable energy, grids and networks*, p. 101580, 2024.
- [22] J. Schulman, F. Wolski, P. Dhariwal, A. Radford, and O. Klimov, "Proximal policy optimization algorithms," *arXiv preprint arXiv:1707.06347*, 2017.
- [23] F. Felten, L. N. Alegre, A. Nowe, A. Bazzan, E. G. Talbi, G. Danoy, and B. C da Silva, "A toolkit for reliable benchmarking and research in multi-objective reinforcement learning," *Advances in Neural Information Processing Systems*, vol. 36, 2024.
- [24] H. Mossalam, Y. M. Assael, D. M. Roijers, and S. Whiteson, "Multi-objective deep reinforcement learning," *arXiv preprint arXiv:1610.02707*, 2016.
- [25] C. F. Hayes, R. Rădulescu, E. Bargiacchi, J. Källström, M. Macfarlane, M. Reymond, T. Verstraeten, L. M. Zintgraf, R. Dazeley, F. Heintz, E. Howley, A. A. Irissappane, P. Mannion, A. Nowé, G. Ramos, M. Restelli, P. Vamplew, and D. M. Roijers, "A practical guide to multi-objective reinforcement learning and planning," *Autonomous Agents and Multi-Agent Systems*, vol. 36, no. 1, 2022.
- [26] RTE France, "Grid2op," 2020. [Online]. Available: <https://github.com/rte-france/Grid2Op>
- [27] D. M. Roijers, "Multi-objective decision-theoretic planning," *AI Matters*, vol. 2, no. 4, pp. 11–12, 2016.
- [28] Delft High Performance Computing Centre (DHPC), "DelftBlue Supercomputer (Phase 2)," <https://www.tudelft.nl/dhpc/ark:/44463/DelftBluePhase2>, 2024.
- [29] T. R. Lautenbacher, A. Rajaei, J. Viebahn, D. Barbieri, and J. Cremer, "Implementation of multi-objective reinforcement learning for power grid topology control," 2025. [Online]. Available: https://github.com/TU-Delft-AI-Energy-Lab/TOPGRID_MORL